# Reduction of interface reactions in low-temperature solid-phase epitaxy of $ScAlMgO_4$ on (0001) $Al_2O_3$

Yajin Chen, Peng Zuo, Yingxin Guan, M. Humed Yusuf, Susan E. Babcock, Thomas F. Kuech. and Paul G. Evans!\*

#### **ABSTRACT**

Low-temperature solid-phase epitaxy is a promising route for the synthesis of thin films of ScAlMgO<sub>4</sub>, a compound with lattice spacings close to compound semiconductors for which there are no practical lattice-matched bulk substrates. Amorphous ScAlMgO<sub>4</sub> films deposited by sputtering on c-plane sapphire, (0001) Al<sub>2</sub>O<sub>3</sub>, were crystallized by subsequent heating. Crystallization at 950 °C resulted in the formation of epitaxial ScAlMgO<sub>4</sub> from the initially amorphous layer over a period of 10 h. The epitaxial film exhibits an epitaxial arrangement in which ScAlMgO<sub>4</sub> [0001] is parallel to Al<sub>2</sub>O<sub>3</sub> [0001] and ScAlMgO<sub>4</sub> [1120] is parallel to Al<sub>2</sub>O<sub>3</sub> [1120]. The as-deposited ScAlMgO<sub>4</sub> films had a non-stoichiometric composition and thus regions of MgAl<sub>2</sub>O<sub>4</sub> were produced during crystallization at 950 °C. Crystallization at a higher temperature, 1400 °C, resulted in unfavorable solid-state reactions between the thin-film and the substrate producing MgAl<sub>2</sub>O<sub>4</sub> and ScAlO<sub>3</sub>.

<sup>&</sup>lt;sup>1</sup> Department of Materials Science and Engineering, University of Wisconsin-Madison, Madison, WI 53706, USA

<sup>&</sup>lt;sup>2</sup> Department of Chemical and Biological Engineering, University of Wisconsin-Madison, Madison, WI 53706, USA

#### INTRODUCTION

Crystalline metal oxides have been used extensively as lattice-matched thin-film or bulk substrates for the synthesis of epitaxial semiconductors.<sup>1-9</sup> Thin-film oxide buffer-layer substrates are particularly useful because complex oxides that are lattice matched with semiconductors can in turn be synthesized as thin films on widely available bulk oxide substrates, such as Al<sub>2</sub>O<sub>3</sub> and yttria-stabilized zirconia (YSZ). For instance, ScAlMgO<sub>4</sub> on a bulk (111) YSZ substrate has served as a lattice-matched buffer layer for the epitaxial growth of both GaN and ZnO.<sup>5, 10, 11</sup> Similarly, a ZnO thin-film on Al<sub>2</sub>O<sub>3</sub> has been used as a lattice-matched buffer layer for the epitaxial growth of GaN.<sup>4</sup> In general, these intermediate crystals have a close lattice match to the semiconductor films and form structurally relaxed layers in which defects arising from the large semiconductor/bulk substrate lattice mismatch can be confined to the buffer layer.

There are several key challenges in the development of oxide thin-film buffer layer substrate for semiconductor epitaxy. Reactions between the buffer layer and substrate can lead to the formation of undesired phases. Solid-state reactions are particularly challenging at high temperatures, for example an undesired MgAl<sub>2</sub>O<sub>4</sub> phase can be formed during the epitaxial crystallization of ScAlMgO<sub>4</sub> buffer layers used for GaN epitaxy. Deposition at high temperatures favors surface atomic mobility, facilitating epitaxy, but simultaneously also increases bulk diffusion leading to the transport of atoms to participate in film/substrate interfacial reactions. Low-temperature epitaxial growth methods can potentially limit the interfacial reaction between film and substrate, thus can expand the range of available oxide substrates for thin-film semiconductor growth. The extent of reactions can be somewhat limited by employing diffusion barriers between the substrate and ScAlMgO<sub>4</sub> layer, by crystallizing amorphous layers via solid-phase epitaxy, or co-depositing compounds serving as crystal growth fluxes. Sind-12 Even with these

steps, however, the use of high temperature processes results in the formation of competing phases. Here we report the development of epitaxial growth methods for ScAlMgO<sub>4</sub> employing solid-phase epitaxy (SPE) at reduced temperatures, permitting epitaxial growth of ScAlMgO<sub>4</sub> on (0001) Al<sub>2</sub>O<sub>3</sub> without an intermediate layer and limiting the formation of undesired phases.

Two methods have been investigated so far to grow ScAlMgO<sub>4</sub> thin films: (i) a variant of SPE incorporating a specially prepared substrate, termed reactive solid-phase epitaxy (R-SPE) and (ii) flux-mediated direct epitaxial growth of ScAlMgO<sub>4</sub>. The R-SPE methods have employed YSZ substrates and involved the crystallization at 1300 to 1500 °C of an amorphous ScAlMgO<sub>4</sub> layer on oxide buffer layers that are consumed by reaction or evaporation during crystallization.<sup>5, 10, 11</sup> The second method involved direct epitaxial growth on (0001) Al<sub>2</sub>O<sub>3</sub> at 840 °C mediated by a bismuth oxide flux.<sup>12</sup> Both of these previous methods face significant challenges. The most important challenge has been that both R-SPE and the direct flux-mediated epitaxy, MgAl<sub>2</sub>O<sub>4</sub> was formed due to reactions between the ScAlMgO<sub>4</sub> film or fluxes and the substrates.<sup>5, 10-12</sup> The origins and consequences of these reactions are slightly different and can be addressed by alternative epitaxial growth strategies.

Several reactions can occur between ScAlMgO<sub>4</sub> and bulk oxide substrates at high temperatures. The formation of epitaxial MgAl<sub>2</sub>O<sub>4</sub> has been observed on (0001) Al<sub>2</sub>O<sub>3</sub> from the MgO-Al<sub>2</sub>O<sub>3</sub> reaction. As we report below, it is also possible to form an ScAlO<sub>3</sub> phase from a reaction between ScAlMgO<sub>4</sub> and Al<sub>2</sub>O<sub>3</sub> at high temperatures. ScAlO<sub>3</sub> has previously been synthesized in the bulk form by a crystallization of amorphous ScAlO<sub>3</sub> at high pressure and recovery to ambient conditions. Nucleation at the interface in the presence of other crystalline phases during SPE may make it possible to form ScAlO<sub>3</sub> via a thin-film reaction. Further reactions are possible on YSZ substrates. In bulk materials, reactions involving Sc can result in the

incorporation of scandium into zirconia, similar to the addition of yttrium into YSZ.<sup>17</sup> The reduction in the Sc content in the film can lead to the formation of the Sc-deficient phases such as MgAl<sub>2</sub>O<sub>4</sub>.<sup>10</sup> Compensation for the loss of Sc by creating a starting amorphous layer with excess Sc, for example by adding 20% excess Sc into the deposition target, reduced the formation of MgAl<sub>2</sub>O<sub>4</sub> when crystallizing ScAlMgO<sub>4</sub> at 1470 °C.<sup>10, 11</sup> However, the film/substrate reaction issue is not solved by this compensation, which only provides enough Sc for both ScAlMgO<sub>4</sub> crystallization and the film/substrate reaction so that MgAl<sub>2</sub>O<sub>4</sub> and an Sc-rich YSZ phase are still formed.

Several indications from previous studies suggest that low-temperature SPE can in principle lead to the crystallization of epitaxial ScAlMgO<sub>4</sub> without unfavorable roughening of the surface or interfacial reactions. The first indications are that the low-temperature regime of SPE has not been fully explored in previous studies and that low-temperatures may offer a favorable combination of reduced reactivity and reduced long-range diffusion. Although the formation of a crystalline ScAlMgO<sub>4</sub> was not observed during direct epitaxy at 700 °C, there was also no interface reaction at that temperature.<sup>5</sup> The specific reactions during flux-mediated epitaxy at the slightly higher temperature 840 °C, apparently involve the flux rather than the substrate and thus also suggest that the extent of the specific ScAlMgO<sub>4</sub>/substrate reaction can be reduced at lower temperatures. <sup>12</sup> Crystallization via R-SPE was observed at lowest temperature previously reported, 1300 °C, but was also accompanied by the development of a three-dimensional crystal morphology at that temperature. 10 The surface and bulk diffusion responsible for large-scale morphological effects and crystal growth can be expected to have different activation energies and it is possible that diffusion will be suppressed as the temperature is decreased before crystallization slows to an impractical speed. A second indication that low-temperature methods may yield a route to the

formation of ScAlMgO<sub>4</sub> without interfacial reactions is that recent results in other compounds indicate that crystal growth via SPE can occur in complex oxides at far lower temperatures than have been previously employed in ScAlMgO<sub>4</sub> epitaxy.<sup>18, 19</sup> SPE in homoepitaxy of SrTiO<sub>3</sub> on SrTiO<sub>3</sub>, for example, occurs at rates on the order of 1 nm min<sup>-1</sup> at 450 °C.<sup>19</sup> Slightly higher temperatures on the order of 800 °C induce heteroepitaxial crystallization in PrAlO<sub>3</sub> on SrTiO<sub>3</sub>.<sup>18</sup> Lower temperatures than have previously been employed in the crystallization of ScAlMgO<sub>4</sub> can in principle simultaneously reduce the rate of interfacial reactions and limit the atomic transport responsible for the development of three-dimensional crystalline morphologies.

We report a low-temperature SPE growth method that enables crystal growth but retains the as-deposited composition of ScAlMgO<sub>4</sub> and alleviates film/substrate interfacial reactions. Amorphous ScAlMgO<sub>4</sub> layers were deposited on (0001) Al<sub>2</sub>O<sub>3</sub> substrates at room temperature and crystallized at elevated temperatures in air. Epitaxial ScAlMgO<sub>4</sub> films in this study were crystallized at 950 °C, a lower temperature than those described in the previous R-SPE processes.<sup>5</sup> Processes. The 950 °C temperature was chosen because an amorphous ScAlMgO<sub>4</sub> film was fully crystallized at this temperature within a relatively short duration of 10 h. A comparison between layers crystallized at 950 °C, and those crystallized at a more conventional temperature 1400 °C, shows that crystallization at high temperatures produces a film/substrate interface reaction yielding several competing phases in addition to ScAlMgO<sub>4</sub>. In addition to the phases previously identified as forming at high temperatures during ScAlMgO<sub>4</sub> epitaxy, we further find that ScAlO<sub>3</sub> was formed from the film/substrate interfacial reaction.

## **EXPERIMENTAL DETAILS**

Thin-films of amorphous ScAlMgO<sub>4</sub> were deposited onto (0001) Al<sub>2</sub>O<sub>3</sub> substrates at room temperature by on-axis radio-frequency magnetron sputtering from an ScAlMgO<sub>4</sub> target (AJA

International, Inc.). The amorphous ScAlMgO<sub>4</sub> layers were grown at a pressure of 18 mTorr in Ar gas at a rate of 13 nm h<sup>-1</sup> and had a nominal total thickness of 50 nm. A second set of ScAlMgO<sub>4</sub> amorphous layers were deposited on silicon substrates with a thin native oxide layer, termed SiO<sub>2</sub>/Si substrates here, under the same deposition conditions in order to measure the composition of the as-deposited films. The solid-phase crystallization of the amorphous ScAlMgO<sub>4</sub> layers was investigated by heating to 950 °C or 1400 °C in a preheated furnace in still air. After crystallization the samples were removed from the furnace and cooled in flowing dry N<sub>2</sub>.

Grazing-incidence X-ray scattering and diffraction studies were conducted using an X-ray diffractometer with Cu K $\alpha$  radiation at a wavelength of 1.54 Å (D8 Discovery, Bruker, Inc.). The X-ray source was operated at 50 kV with an emission current of 1 mA. Studies of the scattering from amorphous layers employed a grazing incident angle 1.4°, which was selected in order to match the X-ray footprint to the overall size of the sample. The distribution of scattered x-rays was measured using a two-dimensional area detector with a conical opening angle of 32°. The center of the detector was positioned at  $2\theta = 30^\circ$  in order to capture the broad distribution of scattered X-ray intensity from the amorphous layers. Studies of the initially amorphous films employed an integration along lines at constant  $2\theta$  in the diffraction pattern. X-ray reflectivity (XRR) measurements of the thickness and roughness of the amorphous layers were performed on a diffractometer employing Cu K $\alpha_1$  X-ray radiation at a wavelength of 1.5406 Å (Panalytical X'Pert MRD).

The epitaxial relationships of between the  $Al_2O_3$  substrate, ScAlMgO<sub>4</sub>, and other phases formed through reactions were determined by using the dependence of the diffracted intensity of thin-film reflections as a function of the rotation of the sample around the surface-normal axis, normally termed a phi scan. Intensities of reflections with the same  $2\theta$  scattering angle were

measured as a function of the azimuthal angle of the sample orientation. A separate series of x-ray measurements were performed on an X-ray diffractometer (Empyrean, Malvern Panalytical, Inc.) equipped with a Cu K $\alpha$ 1 x-ray source with wavelength 1.5406 Å operated at 40 kV and 40 mA.  $\theta$ -2 $\theta$  scans were conducted to identify the crystalline phases formed in the film and to determine the crystal orientation along the out-of-plane direction.

The composition of the ScAlMgO<sub>4</sub> films was probed before crystallization using electronprobe microanalysis with wavelength dispersive X-ray spectroscopy (EPMA-WDS). ScPO<sub>4</sub> and MgAl<sub>2</sub>O<sub>4</sub> were used as reference standards for Sc, Mg, Al and O. Characteristic X-ray intensities from the ScAlMgO<sub>4</sub> thin films and the reference standards were acquired using incident electron energies of 8 and 15 keV. The composition was determined by fitting the spectra acquired at the two incident electron energies to the  $\varphi(\rho z)$  model.<sup>20</sup>

The microstructure of the as-deposited and crystallized ScAlMgO<sub>4</sub> layers on Al<sub>2</sub>O<sub>3</sub> was characterized using STEM. Cross-sectional STEM specimens were prepared using a focused ion beam (FIB) with a Ga ion source operated at 30 kV (Auriga, Zeiss, Inc.). STEM high-angle annular dark-field (HAADF) images and energy-dispersive x-ray spectroscopy (EDS) spectra were collected using an aberration-corrected scanning transmission electron microscope (Titan 80-200, FEI, Inc.) operated at 200 kV with a probe semi-convergence angle of 24.5 mrad and an HAADF detector in the range of 53.9 to 269.5 mrad. The surface of the crystallized layers was characterized using atomic force microscopy (MultiMode 8, Brucker, Inc.) in a non-contact imaging mode.

## **RESULTS**

X-ray scattering studies showed that the as-deposited ScAlMgO<sub>4</sub> films were amorphous. Fig. 1(a) shows X-ray scattering patterns from an as-deposited ScAlMgO<sub>4</sub> layer on Al<sub>2</sub>O<sub>3</sub> and from an Al<sub>2</sub>O<sub>3</sub> substrate without a thin film layer. Two broad intensity maxima at  $2\theta = 32^{\circ}$  and  $42^{\circ}$  arise

from the as-deposited ScAlMgO<sub>4</sub> thin layer, consistent with an amorphous structure. The angular widths of the two amorphous intensity maxima in Fig. 1(a) differ because these two peaks arise from cation-oxygen and cation-cation pairs, respectively, and the range of ionic separations in these pairs is different. The spacings can be estimated using the structure of crystalline ScAlMgO<sub>4</sub> phase, in which the cation-oxygen spacing to the next-neighbor varies from Al (or Mg)-O 1.89 Å to Sc-O 2.15 Å. The cation-cation spacing to the next neighbor varies in a larger range: from Al (or Mg)-Al (or Mg) 3.03 Å to Sc-Al (or Mg) 3.53 Å.21 The larger spread of cation-cation separations gives rise to a broader amorphous peak at  $2\theta = 32^{\circ}$  and the cation-oxygen separations produce the narrower peak at  $2\theta = 42^{\circ}$ . The Al<sub>2</sub>O<sub>3</sub> substrate exhibits a featureless low-intensity distribution of scattered x-ray intensity. The XRR intensity distribution measured with the asdeposited ScAlMgO<sub>4</sub> layer is shown in Fig. 1(b). The fit of a single-layer x-ray reflectivity model gives an as-deposited thickness of 48 nm and root-mean-square roughness of 1.6 nm. The EPMA-WDS analysis reveals that the as-deposited ScAlMgO<sub>4</sub> layers are non-stochiometric. The ScAlMgO<sub>4</sub> thin film deposited on an SiO<sub>2</sub>/Si substrate does not exhibit Al signal that would otherwise arise from an Al<sub>2</sub>O<sub>3</sub> substrate, allowing the Al composition to be measured more precisely. The ScAlMgO<sub>4</sub>/SiO<sub>2</sub>/Si sample has an Sc:Al:Mg atomic ratio of 1.0:1.1:1.2.

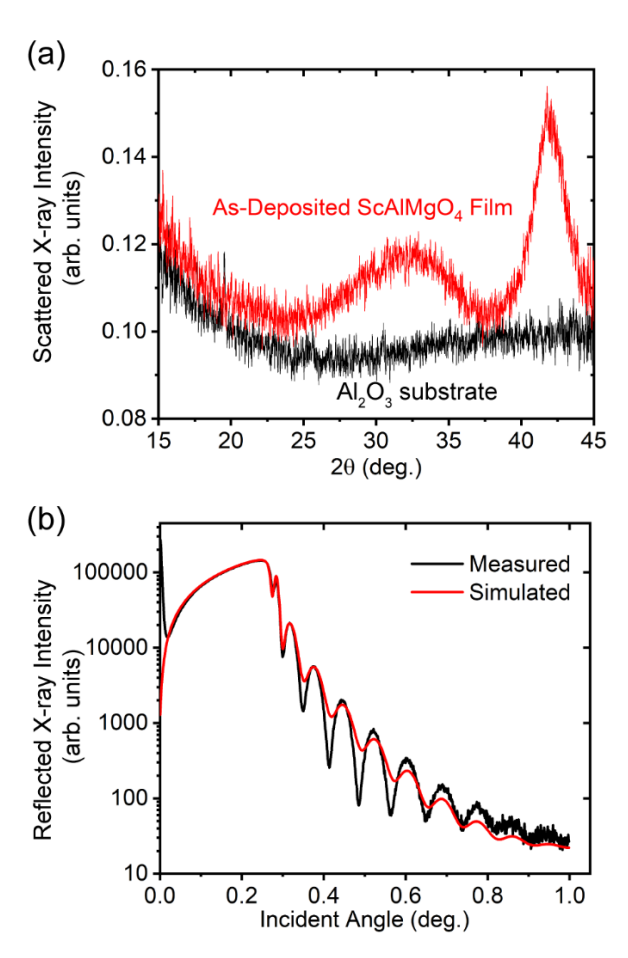


Figure 1. (a) Grazing-incidence X-ray scattering patterns of an as-deposited ScAlMgO<sub>4</sub> layer on (0001) Al<sub>2</sub>O<sub>3</sub> (red) and an (0001) Al<sub>2</sub>O<sub>3</sub> substrate without a film (black). The broad scattering intensity maxima at 32° and 42° arise from the amorphous ScAlMgO<sub>4</sub> film. (b) X-ray reflectivity distribution from the as-deposited amorphous ScAlMgO<sub>4</sub> film (black) and fit of a single-layer x-ray reflectivity model with thickness 48 nm and root-mean-square roughness 1.6 nm.

We hypothesize that the formation of ScAlMgO<sub>4</sub> during the crystallization of the amorphous layer consumes all of the available Sc. The remaining materials would then correspond to a composition ratio Mg:Al 2:1. This composition lies in the MgO plus MgAl<sub>2</sub>O<sub>4</sub> phase field of the equilibrium Mg-Al-O phase diagram for temperatures in the range 950 °C to 1400 °C.<sup>22</sup> In this composition range, MgO can also react with the Al<sub>2</sub>O<sub>3</sub> substrate to form MgAl<sub>2</sub>O<sub>4</sub>.<sup>22</sup> We thus expect that the phase formed in addition to ScAlMgO<sub>4</sub> in the layers with the composition we have deposited will be MgAl<sub>2</sub>O<sub>4</sub>, the Mg-Al spinel phase.

A θ-2θ diffraction pattern of an ScAlMgO<sub>4</sub> thin film crystallized at 950 °C for 10 h is

shown in Fig. 2(a). The thin-film diffraction peaks observed in Fig. 2(a) can be indexed using the reported structures of ScAlMgO<sub>4</sub> and MgAl<sub>2</sub>O<sub>4</sub>.  $^{21,23}$  The ScAlMgO<sub>4</sub> (0009) reflection at  $2\theta = 32^{\circ}$  in Fig. 2(a) corresponds to a c lattice parameter of 25.2 Å, matching the reported bulk ScAlMgO<sub>4</sub> lattice parameter c = 25.15 Å.  $^{21}$  The MgAl<sub>2</sub>O<sub>4</sub> 111 and 311 reflections in Fig. 2(a) indicate that MgAl<sub>2</sub>O<sub>4</sub> crystalizes in two different orientations: (i) with MgAl<sub>2</sub>O<sub>4</sub> [111] parallel to Al<sub>2</sub>O<sub>3</sub> [0001] and (ii) MgAl<sub>2</sub>O<sub>4</sub> [311] parallel to Al<sub>2</sub>O<sub>3</sub> [0001]. The stronger MgAl<sub>2</sub>O<sub>4</sub> 004 reflection is not observed in Fig. 2(a), indicating that the MgAl<sub>2</sub>O<sub>4</sub> film has a crystalline texture with these preferred orientations. The X-ray  $\theta$ -2 $\theta$  scan pattern in Fig. 2(a) shows that the ScAlMgO<sub>4</sub> [0001] direction is aligned with the [0001] direction of the Al<sub>2</sub>O<sub>3</sub> substrate. The rocking curve of the ScAlMgO<sub>4</sub> 0009 reflection has a full-width at half-maximum (FWHM) of 0.9°, as shown in Fig. 2(b). Heating to 950 °C for 5 h resulted in the partial crystallization of ScAlMgO<sub>4</sub>. Heating to 900 °C for a longer duration, 48 h, also resulted a fully crystallized ScAlMgO<sub>4</sub> layer.

Further information about the epitaxial relationship between ScAlMgO<sub>4</sub> and the Al<sub>2</sub>O<sub>3</sub> substrate was obtained using azimuthal X-ray diffraction scans. Fig. 2(c) shows the azimuthal angle dependence of the intensities of reflection in three families of planes: Al<sub>2</sub>O<sub>3</sub> {11 $\bar{2}$ 3}, ScAlMgO<sub>4</sub> {11 $\bar{2}$ 6}, and ScAlMgO<sub>4</sub> {01 $\bar{1}$ 5}. As illustrated in Fig. 2(c), all of these have six-fold symmetry and the ScAlMgO<sub>4</sub> {11 $\bar{2}$ 6} reflections appear at the same azimuthal angles as the Al<sub>2</sub>O<sub>3</sub> {11 $\bar{2}$ 3} reflections. The ScAlMgO<sub>4</sub> {01 $\bar{1}$ 5} reflections are rotated by 30° in the azimuthal angle from the Al<sub>2</sub>O<sub>3</sub> {11 $\bar{2}$ 3} reflections. The epitaxial relationship between the ScAlMgO<sub>4</sub> film and the Al<sub>2</sub>O<sub>3</sub> substrate is thus ScAlMgO<sub>4</sub> [0001] is parallel to Al<sub>2</sub>O<sub>3</sub> [0001] and ScAlMgO<sub>4</sub> [11 $\bar{2}$ 0] parallel to Al<sub>2</sub>O<sub>3</sub> [11 $\bar{2}$ 0].

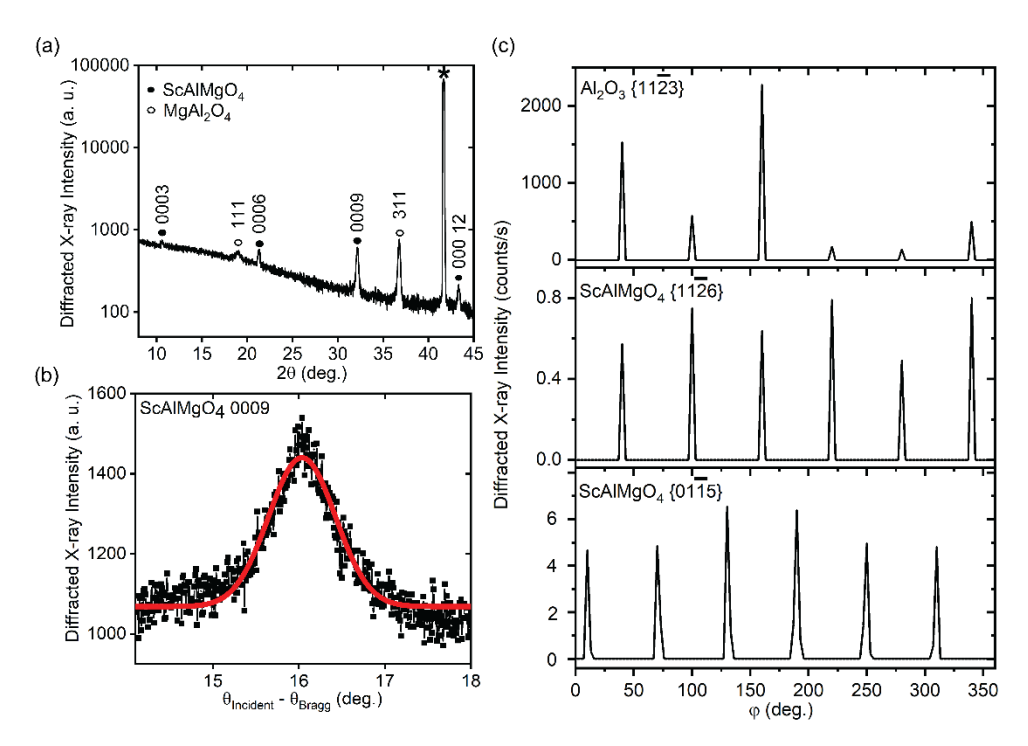


Figure 2. (a) X-ray  $\theta$ -2 $\theta$  diffraction pattern of an ScAlMgO<sub>4</sub> film crystallized at 950 °C for 10 h. The Al<sub>2</sub>O<sub>3</sub> 0006 reflection is marked with an asterisk. (b) Rocking curve (black) of the ScAlMgO<sub>4</sub> 0009 reflection with FWHM of 0.9° derived from the Gaussian fit (red). (c) Azimuthal angle dependence of the diffracted X-ray intensity from Al<sub>2</sub>O<sub>3</sub> {11 $\bar{2}$ 3}, ScAlMgO<sub>4</sub> {11 $\bar{2}$ 6} and ScAlMgO<sub>4</sub> {01 $\bar{1}$ 5}.

A cross-sectional STEM-HAADF image of an ScAlMgO<sub>4</sub> layer crystallized at 950 °C for 10 h is shown in Fig. 3(b). The absolute scattered electron intensity in the STEM-HAADF measurement is approximately proportional to the square of the atomic number (Z) averaged along the column illuminated by the scanning electron beam.<sup>24</sup> To identify the phases from the STEM-HAADF image, it is useful to consider the volume-averaged values of Z<sup>2</sup> for the compounds appearing in the x-ray diffraction patterns: ScAlMgO<sub>4</sub>, Al<sub>2</sub>O<sub>3</sub>, and MgAl<sub>2</sub>O<sub>4</sub>. We exclude the oxygen atoms from these calculations because their small atomic number leads to very low scattered electron intensities. The volume averaged values of Z<sup>2</sup> (excluding oxygen) based on the reported structures of these compounds are 9.9 e-<sup>2</sup>/Å<sup>3</sup> for ScAlMgO<sub>4</sub>, 8.0 e-<sup>2</sup>/Å<sup>3</sup> for Al<sub>2</sub>O<sub>3</sub>, and 7.3 e-<sup>2</sup>/Å<sup>3</sup> for MgAl<sub>2</sub>O<sub>4</sub>.<sup>21,23,25</sup> Assuming constant specimen thickness, regions of ScAlMgO<sub>4</sub> produce higher scattered electron intensity than Al<sub>2</sub>O<sub>3</sub>, which in turn is slightly more intense than MgAl<sub>2</sub>O<sub>4</sub>.

The intensity contrast between the substrate and the film in Fig. 3(b) indicates that the composition of the thin film crystallized at 950  $^{\circ}$ C is predominantly ScAlMgO<sub>4</sub> and that there is an abrupt boundary between ScAlMgO<sub>4</sub> layer and the Al<sub>2</sub>O<sub>3</sub> substrate. No clear film/substrate reaction is found in the intensity analysis at the film/substrate interface.

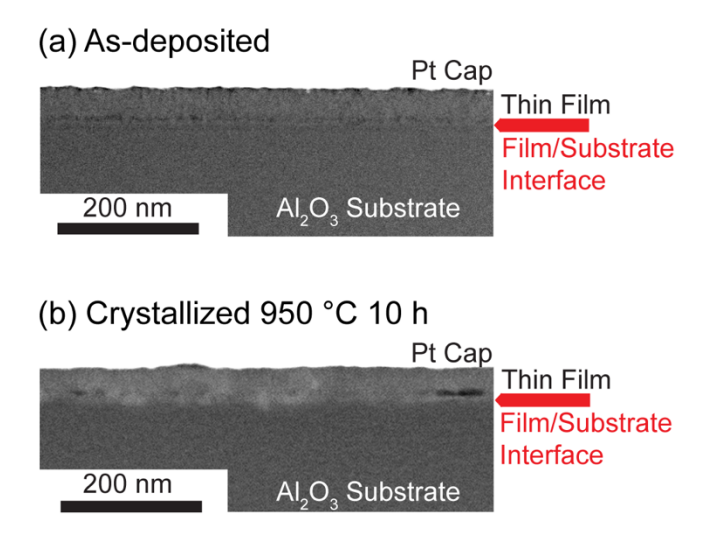


Figure 3. STEM-HAADF images of (a) the as-deposited amorphous ScAlMgO<sub>4</sub> film and (b) the ScAlMgO<sub>4</sub> film crystallized at 950 °C for 10 h. The film/substrate interfaces are indicated by arrows.

An artifact linked to the deposition of the ScAlMgO<sub>4</sub> is apparent in both the as-deposited layer in Fig. 3(a) and the crystallized layer in Fig. 3(b). A line of isolated regions of low scattered electron intensity appears at a distance of 4 nm from the film/substrate interface in the as-deposited film in Fig. 3(a). The intensity analysis shows the scattered intensity from this dark line is 10% lower than the Al<sub>2</sub>O<sub>3</sub> substrate, which suggests that this region is composed of a layer enriched in in Mg and Al. The same layer is also apparent as a region of darker contrast within the film after crystallization at 950 °C for 10 h in Fig. 3(b). The presence of the light elements rich layer in the as-deposited film could in principle be related to variation in the deposition parameters during the sputtering of the amorphous layer.

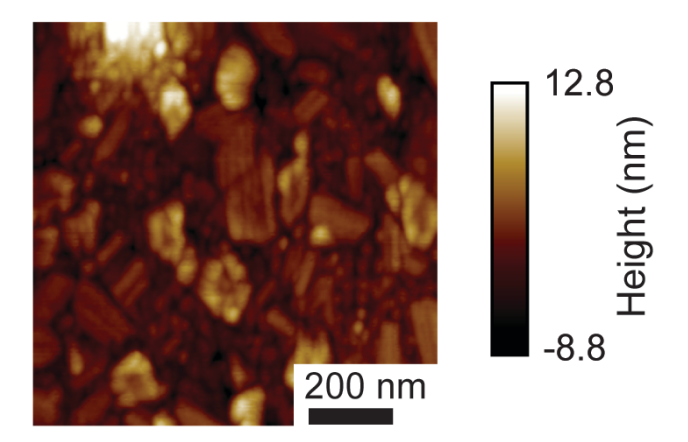


Figure 4. AFM image of an ScAlMgO<sub>4</sub> film crystallized at 950 °C for 10 h. The root-mean-square surface roughness is 2.95 nm.

The surface morphology of the ScAlMgO<sub>4</sub> film crystallized at 950 °C for 10 h was characterized using AFM. As apparent in the AFM image in Fig. 4, the surface has features consistent with the existence of many crystallites with nm-scale surface-height differences. The surface has a root-mean-square roughness of 2.95 nm. The distribution of the crystallites is consistent with the formation of the MgAl<sub>2</sub>O<sub>4</sub> phase during crystallization due to the non-stoichiometry of the as-deposited amorphous ScAlMgO<sub>4</sub>.

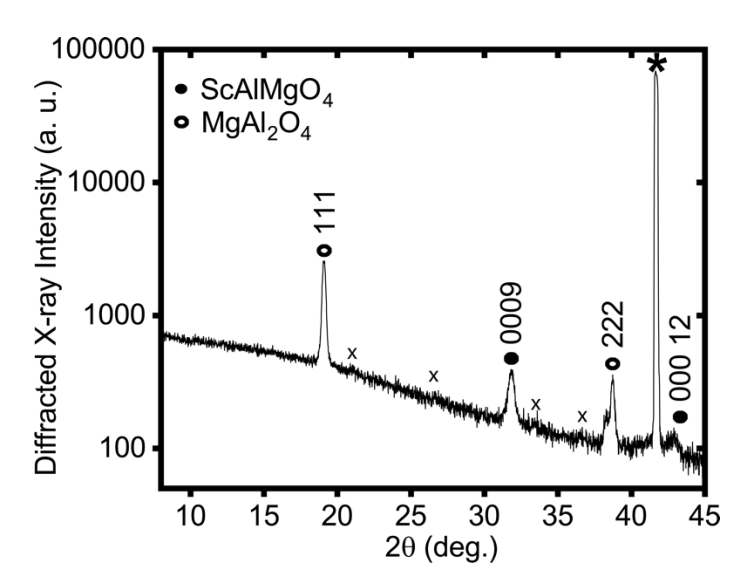


Figure 5. X-ray  $\theta$ -2 $\theta$  diffraction pattern of an ScAlMgO<sub>4</sub> film crystallized at 1400 °C for 30 min. The Al<sub>2</sub>O<sub>3</sub> substrate 0006 reflection is marked with an asterisk. Angles of possible weak reflections from ScAlO<sub>3</sub> are indicated with "x".

Crystallization at a higher temperature, 1400 °C, results in several solid-state reactions. The θ-2θ X-ray diffraction pattern of ScAlMgO<sub>4</sub> crystallized at 1400 °C is shown in Fig. 5. As was the case following crystallization at 950 °C, both ScAlMgO<sub>4</sub> and MgAl<sub>2</sub>O<sub>4</sub> are observed in the diffraction pattern. Crystallization at 1400 °C produces stronger MgAl<sub>2</sub>O<sub>4</sub> {111}-family x-ray reflections than were observed in the layer crystallized at 950 °C. The cross-sectional STEM-HAADF image of the sample crystalized at 1400 °C in Fig. 6(a) provides information about the extent of the solid-state reaction. Regions of higher scattered electron intensity in Fig. 6(a) extend into the substrate in spatially isolated areas. EDS measurements indicate that the intensity variation in Fig. 6(a) arises from compositional differences within the crystallized film after heating to 1400 °C. EDS spectra acquired at two locations are shown in Figs. 6(b) and (c). The spectrum acquired from an area of high scattered electron intensity, Fig. 6(b), exhibits peaks from the fluorescence of Sc, Al and O but not Mg. The quantification of this EDS spectrum shows an approximate composition of Sc 21 at%, Al 34 at% and O 45 at%, consistent with the formation of ScAlO<sub>3</sub> within the measurement uncertainty given the unknown contribution of Al<sub>2</sub>O<sub>3</sub> substrate to the EDS spectrum. Bulk ScAlO<sub>3</sub> has an orthorhombic crystal structure with a = 4.935 Å, b = 5.230 Å, and c = 7.201 Å. The locations of possible weak x-ray reflections at angles corresponding to the ScAlO<sub>3</sub> orthorhombic structures are indicated in the X-ray  $\theta$ -2 $\theta$  diffraction pattern in Fig. 5. The second region of the film analyzed with EDS exhibits the spectrum shown in Fig. 6(c) and has approximate composition Mg 15 at%, Al 53 at%, and O 32 at%, consistent with the MgAl<sub>2</sub>O<sub>4</sub> phase, again within the uncertainty arising due to the proximity of the Al<sub>2</sub>O<sub>3</sub> substrate.

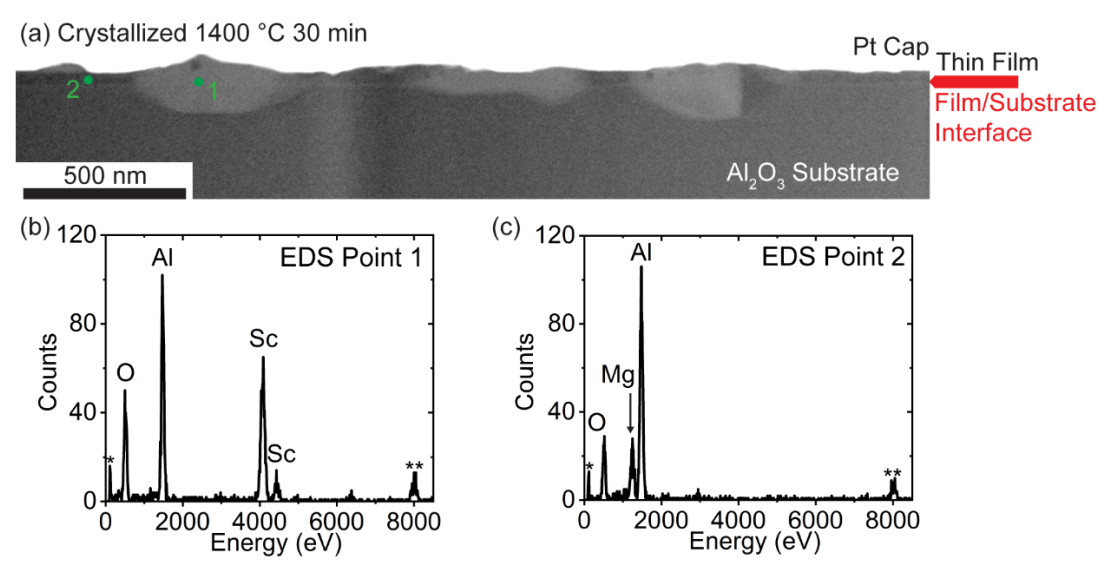


Figure 6. (a) STEM-HAADF image of an ScAlMgO<sub>4</sub> film after crystallization at 1400°C for 30 min. EDS spectra collected points (b) 1 and (c) 2. EDS artifacts arise from the Be sample holder (\*) and Cu in the STEM specimen grid (\*\*).

## **DISCUSSION**

The extension of crystallization to lower temperatures appears to be enabled by the differences in the reported activation energies of key kinetic steps.<sup>26</sup> Precise measurements and theoretical predictions are not yet available for the kinetics of ScAlMgO<sub>4</sub> crystallization, atomic transport on ScAlMgO<sub>4</sub>, or reactions in the Sc-Al-Mg-O system. Some insight can be gained, however, by considering the reported activation energies of the relevant processes in similar systems. The activation energy for crystallization has been previously reported for SrTiO<sub>3</sub>, a prototypical complex oxide. These studies indicate that the crystallization process occurs with an activation energy of 0.7 to 1 eV and that the precise value of the energy depends on the gas environment.<sup>19, 27-29</sup> The rate of chemical reaction at interfaces depends on the detailed rate of the specific reaction and on diffusive flux of reacting atoms to the interface. The high-temperature results here, and in previous studies, <sup>5, 10, 11</sup> show that the interface reaction is favorable and thus suggest that limiting atomic diffusion is crucial in reducing the formation of competing phases. Although self-diffusion rates have not yet been measured for ScAlMgO<sub>4</sub>, activation energies for

diffusion in other compounds are available for comparison. The activation energies for self-diffusion of Al and O in Al<sub>2</sub>O<sub>3</sub> are both higher than 1 eV.<sup>30</sup> The evolution of the crystal morphology towards the complex structures previously reported for ScAlMgO<sub>4</sub> depends on surface diffusion. Activation energies for surface diffusion have been reported for the compounds SrRuO<sub>3</sub>, SrTiO<sub>3</sub>, and YBa<sub>2</sub>Cu<sub>3</sub>O<sub>7</sub> are all higher than 1 eV.<sup>31,32</sup> The relative importance of bulk and surface diffusion can thus be expected to decrease faster than crystallization as the temperature is decreased. This favorable combination of activation energies is consistent with the experimental results reported here and also suggests that SPE can in principle reduce the impact of interfacial reactions and morphologies leading to rough surfaces in other chemically complex oxides.

The low-temperature process alleviates film/substrate reactions that have been previously observed in the ScAlMgO<sub>4</sub> growth at high-temperature.<sup>5, 10, 11</sup> In addition to the previously reported formation of MgAl<sub>2</sub>O<sub>4</sub> phase, the STEM micrographs indicate that ScAlO<sub>3</sub> can be formed at high temperature via reactions during ScAlMgO<sub>4</sub> SPE. Previous studies of ScAlO<sub>3</sub> with bulk synthesis at atmospheric pressure have produced amorphous ScAlO<sub>3</sub> and have required high-pressure processing to yield the crystalline phase.<sup>33</sup> The development of regions of ScAlO<sub>3</sub> in reactions with ScAlMgO<sub>4</sub> shows that this phase must also be considered in the analysis of the phenomena limiting the temperature regime available for SPE. More generally, the formation of ScAlO<sub>3</sub> in this study shows that SPE can lead to the nucleation of compounds that that are otherwise not accessible through bulk ambient-pressure synthesis.

The c-axis lattice parameter of ScAlMgO<sub>4</sub> layers crystallized at 950 °C is very close to the value reported for bulk ScAlMgO<sub>4</sub> crystals. The epitaxial strain due to the large lattice mismatch between ScAlMgO<sub>4</sub> and Al<sub>2</sub>O<sub>3</sub> layers is thus relaxed, leaving the ScAlMgO<sub>4</sub> with a surface lattice parameter favorable for the subsequent growth of GaN and other lattice-matched semiconductors.

## **CONCLUSION**

These results indicate that there is a temperature regime in which ScAlMgO<sub>4</sub> thin films can be crystallized via SPE without the interfacial reactions and complex crystalline morphologies that emerge at high temperatures. The discovery of this regime of crystallization is consistent with the differences among activation energies for crystallization, bulk diffusion, and surface diffusion. The temperature dependence of the crystallization and reaction processes can in principle be used to measure the relevant activation energies of several important kinetic phenomena and establish the precise regime in which ScAlMgO<sub>4</sub> can be crystallized while avoiding interfacial reactions. The expanded temperature range applicable to the formation of ScAlMgO<sub>4</sub> shows that processes incorporating SPE can be optimized to yield ScAlMgO<sub>4</sub> buffer layers with structure and morphology compatible with the subsequent epitaxial growth of semiconductors.

#### **AUTHOR INFORMATION**

## **Corresponding Author**

\* E-mail: pgevans@wisc.edu. Address: Department of Materials Science and Engineering,
University of Wisconsin-Madison, 1105 Engineering Research Building, 1500 Engineering Dr.,
Madison, WI 53706, USA

## **Present Addresses**

Yajin Chen, Stanford Synchrotron Radiation Light Source, SLAC National Accelerator Laboratory, Menlo Park, CA 94025, USA; M. Humed Yusuf, Intel Corporation, Hillsboro, OR 97124, USA.

## **Author Contributions**

YC and MHY deposited the amorphous films and crystallized the deposited layers. YC and PZ performed the X-ray diffraction measurements. PZ, YG, and SEB conducted the STEM experiments. All authors contributed to the preparation of the manuscript. All authors have given approval to the final version of the manuscript.

## **Funding Sources**

This research work was primarily funded by the NSF Division of Materials Research through the University of Wisconsin Materials Research Science and Engineering Center (grant DMR-1720415).

### **Notes**

The authors declare no competing financial interest.

## **ACKNOWLEDGMENT**

The authors gratefully acknowledge Dr. J. H. Fournelle in the Department of Geoscience at University of Wisconsin-Madison for the SEM-EDS measurements and the EPMA-WDS measurements.

## **ABBREVIATIONS**

YSZ, yttria-stabilized zirconia; SPE, solid-phase epitaxy; R-SPE, reactive solid-phase epitaxy; XRR, x-ray reflectivity; STEM, scanning transmission electron microscopy; EPMA-WDS, electron-probe microanalysis with wavelength dispersive X-ray spectroscopy; FIB, focused ion beam; HAADF, high-angle annular dark-field; EDS, energy-dispersive X-ray spectroscopy; AFM, atomic force microscopy.

#### REFERENCES

- 1. Li, N.; Wang, S.-J.; Park, E.-H.; Feng, Z. C.; Tsai, H.-L.; Yang, J.-R.; Ferguson, I., Suppression of Phase Separation in InGaN Layers Grown on Lattice-Matched ZnO Substrates. *J. Cryst. Growth* **2009**, 311, 4628-4631.
- 2. Okazaki, H.; Arakawa, A.; Asahi, T.; Oda, O.; Aiki, K., GaN Epitaxial Growth on Neodium Gallate Substrates. *Solid-State Electron.* **1997,** 41, 263-266.
- 3. Makino, T.; Tamura, K.; Chia, C. H.; Segawa, Y.; Kawasaki, M.; Ohtomo, A.; Koinuma, H., Photoluminescence Properties of ZnO Epitaxial Layers Grown on Lattice-Matched ScAlMgO<sub>4</sub> Substrates. *J. Appl. Phys.* **2002**, 92, 7157-7159.
- 4. Detchprohm, T.; Amano, H.; Hiramatsu, K.; Akasaki, I., The Growth of Thick GaN Film on Sapphire Substrate by Using ZnO Buffer Layer. *J. Cryst. Growth* **1993**, 128, 384-390.
- 5. Katase, T.; Nomura, K.; Ohta, H.; Yanagi, H.; Kamiya, T.; Hirano, M.; Hosono, H., Fabrication of ScAlMgO<sub>4</sub> Epitaxial Thin Films Using ScGaO<sub>3</sub>(ZnO)<sub>m</sub> Buffer Layers and Its Application to Lattice-Matched Buffer Layer for ZnO Epitaxial Growth. *Thin Solid Films* **2008**, 516, 5842-5846.
- 6. Reed, M. D.; Kryliouk, O. M.; Mastro, M. A.; Anderson, T. J., Growth and Characterization of Single-Crystalline Gallium Nitride Using (100) LiAlO<sub>2</sub> Substrates. *J. Cryst. Growth* **2005**, 274, 14-20.
- 7. Hellman, E. S.; Brandle, C. D.; Schneemeyer, L. F.; Wiesmann, D.; Brener, I.; Siegrist, T.; Berkstresser, G. W.; Buchanan, D. N. E.; Hartford, E. H., ScAlMgO<sub>4</sub>: An Oxide Substrate for GaN Epitaxy. *MRS Internet J. Nitride Semicond. Res.* **1996,** 1, U3-U13.

- 8. Ohtomo, A.; Tamura, K.; Saikusa, K.; Takahashi, K.; Makino, T.; Segawa, Y.; Koinuma, H.; Kawasaki, M., Single Crystalline ZnO Films Grown on Lattice-Matched ScAlMgO4(0001) Substrates. *Appl. Phys. Lett.* **1999**, 75, 2635-2637.
- 9. Gu, S.; Zhang, R.; Sun, J.; Zhang, L.; Kuech, T. F., Role of Interfacial Compound Formation Associated with the Use of ZnO Buffers Layers in the Hydride Vapor Phase Epitaxy of GaN. *Appl. Phys. Lett.* **2000**, 76, 3454-3456.
- 10. Katase, T.; Nomura, K.; Ohta, H.; Yanagi, H.; Kamiya, T.; Hirano, M.; Hosono, H., Large Domain Growth of GaN Epitaxial Films on Lattice-Matched Buffer Layer ScAlMgO<sub>4</sub>. *Mater. Sci. Eng., B* **2009**, 161, 66-70.
- 11. Katase, T.; Nomura, K.; Ohta, H.; Yanagi, H.; Kamiya, T.; Hirano, M.; Hosono, H., Fabrication of Atomically Flat ScAlMgO<sub>4</sub> Epitaxial Buffer Layer and Low-Temperature Growth of High-Mobility ZnO Films. *Cryst. Growth Des.* **2010**, 10, 1084-1089.
- 12. Obata, T.; Takahashi, R.; Ohkubo, I.; Oshima, M.; Nakajima, K.; Chikyow, T.; Koinuma, H.; Matsumoto, Y., Epitaxial ScAlMgO<sub>4</sub>(0001) Films Grown on Sapphire Substrates by Flux-Mediated Epitaxy. *Appl. Phys. Lett.* **2006**, 89, 2387124.
- 13. Liu, C.-M.; Chen, J.-C.; Chen, C.-J., The Growth of An Epitaxial Mg–Al Spinel Layer on Sapphire by Solid-State Reactions. *J. Cryst. Growth* **2005**, 285, 275-283.
- 14. Kumar, P.; Dregia, S. A.; Sandhage, K. H., Epitaxial Growth of Magnesia and Spinel on Sapphire during Incongruent Reduction in Molten Magnesium. *J. Mater. Res.* **1999**, 14, 3312-3318.
- 15. Liebermann, R. C.; Jones, L. E. A.; Ringwood, A. E., Elasticity of Aluminate, Titanate, Stannate and Germanate Compounds with the Perovskite Structures. *Phys. Earth Planet*.

Inter. 1977, 14, 165-178.

- 16. Hill, R. J.; Jackson, I., The Thermal Expansion of ScAlO<sub>3</sub> A Silicate Perovskite Analogue. *Phys. Chem. Miner.* **1990,** 17, 89-96.
- 17. Badwal, S. P. S.; Ciacchi, F. T.; Rajendran, S.; Drennan, J., An Investigation of Conductivity, Microstructure and Stability of Electrolyte Compositions in the System 9 mol% (Sc<sub>2</sub>O<sub>3</sub>-Y<sub>2</sub>O<sub>3</sub>)-ZrO<sub>2</sub>(Al<sub>2</sub>O<sub>3</sub>). *Solid State Ionics* **1998**, 109, 167-186.
- 18. Waduge, W. L. I.; Chen, Y.; Zuo, P.; Jayakodiarachchi, N.; Kuech, T. F.; Babcock, S. E.; Evans, P. G.; Winter, C. H., Solid-Phase Epitaxy of Perovskite High Dielectric PrAlO<sub>3</sub> Films Grown by Atomic Layer Deposition for Use in Two-Dimensional Electronics and Memory Devices. *ACS Appl. Nano Mater.* **2019**, 2, 7449-7458.
- 19. Chen, Y. J.; Yusuf, M. H.; Guan, Y. X.; Jacobson, R. B.; Lagally, M. G.; Babcock, S. E.; Kuech, T. F.; Evans, P. G., Distinct Nucleation and Growth Kinetics of Amorphous SrTiO<sub>3</sub> on (001) SrTiO<sub>3</sub> and SiO<sub>2</sub>/Si: A Step toward New Architectures. *ACS Appl. Mater. Interf.* **2017**, 9, 41034-41042.
- 20. Moy, A.; Fournelle, J., Modern Thin Film Analysis by Electron Probe Microanalysis. 2019 MAS Quantitative Microanalysis Topical Conference 2019, pp 64-65.
- 21. Kimizuka, N.; Mohri, T., Structural Classification of RAO<sub>3</sub>(MO)<sub>n</sub> Compounds (R = Sc, In, Y, or Lanthanides; A = Fe(III), Ga, Cr, or Al; M = Divalent Cation; n = 1-11). *J. Solid State Chem.* **1989**, 78, 98-107.
- 22. Hallstedt, B., Thermodynamic Assessment of the System MgO-Al<sub>2</sub>O<sub>3</sub>. *J. Am. Ceram. Soc.* **1992**, 75, 1497-1507.
  - 23. Zorina, N. G.; Kvitka, S. S., Refinement of the Structure of the Spinel Al<sub>2</sub>MgO<sub>4</sub>.

*Kristallografiya* **1969,** 13, 703-705.

- 24. Hartel, P.; Rose, H.; Dinges, C., Conditions and Reasons for Incoherent Imaging in STEM. *Ultramicroscopy* **1996**, 63, 93-114.
- 25. Swanson, H. E.; Fuyat, R. K., *National Bureau of Standards (U. S.) Circular 539*.U. S. Department of Commerce, National Bureau of Standards, 1953.
- 26. Evans, P. G.; Chen, Y. J.; Tilka, J. A.; Babcock, S. E.; Kuech, T. F., Crystallization of Amorphous Complex Oxides: New Geometries and New Compositions via Solid Phase Epitaxy. *Curr. Opin. Solid State Mater. Sci.* **2018**, 22, 229-242.
- 27. White, C. W.; Boatner, L. A.; Sklad, P. S.; Mchargue, C. J.; Rankin, J.; Farlow, G. C.; Aziz, M. J., Ion-Implantation and Annealing of Crystalline Oxides and Ceramic Materials. *Nucl. Instrum. Meth. B* **1988**, 32, 11-22.
- 28. Rankin, J.; McCallum, J. C.; Boatner, L. A., The Effect of Annealing Environments on the Epitaxial Recrystallization of Ion-Beam-Amorphized SrTiO<sub>3</sub>. *J. Mater. Res.* **1992,** 7, 717-724.
- 29. Simpson, T. W.; Mitchell, I. V.; Mccallum, J. C.; Boatner, L. A., Hydrogen Catalyzed Crystallization of Strontium Titanate. *J. Appl. Phys.* **1994,** 76, 2711-2718.
- 30. Pan, J.; Öijerholm, J.; Belonoshko, A. B.; Rosengren, A.; Leygraf, C., Self-diffusion Activation Energies in α-Al<sub>2</sub>O<sub>3</sub> below 1000 °C Measurements and Molecular Dynamics Calculation. *Phil. Mag. Lett.* **2004**, 84, 781-789.
- 31. Dam, B.; Stauble-Pumpin, B., Growth Mode Issues in Epitaxy of Complex Oxide Thin Films. *J. Mater. Sci.-Mater. Electron.* **1998,** 9, 217-226.
  - 32. Rijnders, G.; Blank, D. H. A.; Choi, J.; Eom, C. B., Enhanced Surface Diffusion

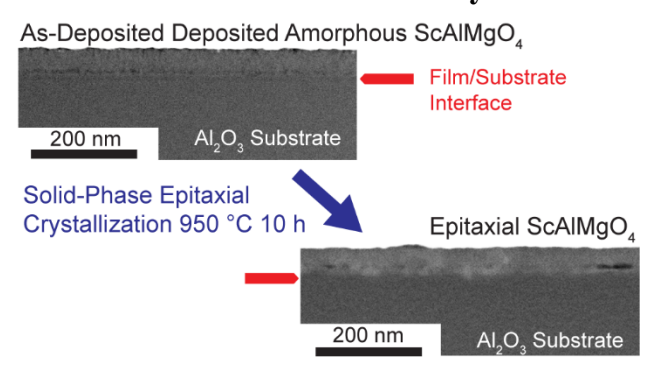
through Termination Conversion during Epitaxial SrRuO<sub>3</sub> Growth. *Appl. Phys. Lett.* **2004,** 84, 505-507.

33. Reid, A. F.; Ringwood, A. E., High-Pressure Modification of ScAlO<sub>3</sub> and Some Geophyiscal Implications. *J. Geophys. Res.* **1975**, 80, 3363-3370.

# Reduction of interface reactions in low-temperature solid-phase epitaxy of ScAlMgO $_4$ on (0001) Al $_2$ O $_3$

Yajin Chen, Peng Zuo, Yingxin Guan, M. Humed Yusuf, Susan E. Babcock, Thomas F. Kuech, and Paul G. Evans!\*

## For Table of Contents Use Only



# **Synopsis:**

Crystallization at a relatively low temperature allows ScAlMgO<sub>4</sub> epitaxial thin films to be synthesized by solid-phase epitaxy, avoiding a film/substrate reaction observed at higher temperatures. Epitaxial ScAlMgO<sub>4</sub> was formed on Al<sub>2</sub>O<sub>3</sub> substrates at 950 °C, while interface reactions are observed during high-temperature crystallization processes. The layers hold promise as lattice-matched substrates for semiconductor epitaxy.

<sup>&</sup>lt;sup>1</sup> Department of Materials Science and Engineering, University of Wisconsin-Madison, Madison, WI 53706, USA

<sup>&</sup>lt;sup>2</sup> Department of Chemical and Biological Engineering, University of Wisconsin-Madison, Madison, WI 53706, USA